archives
of thermodynamics
Vol. **35**(2014), No. 4, 3–27
DOI: 10.2478/aoter-2014-0030

Condensation enhancement by means of electrohydrodynamic techniques

DARIUSZ BUTRYMOWICZ[a*]
JAROSŁAW KARWACKI[b]
MARIAN TRELA[b]

[a] Bialystok University of Technology, Wiejska 45A, 15-351 Bialystok, Poland

[b] The Szewalski Institute of Fluid-Flow Machinery, Polish Academy of Sciences, Fiszera 14, 80-231 Gdańsk, Poland

Abstract Short state-of-the-art on the enhancement of condensation heat transfer techniques by means of condensate drainage is presented in this paper. The electrohydrodynamic (EHD) technique is suitable for dielectric media used in refrigeration, organic Rankine cycles and heat pump devices. The electric field is commonly generated in the case of horizontal tubes by means of a rod-type electrode or mesh electrodes. Authors proposed two geometries in the presented own experimental investigations. The first one was an electrode placed just beneath the tube bottom and the second one consisted of a horizontal finned tube with a double electrode placed beneath the tube. The experimental investigations of these two configurations for condensation of refrigerant R-123 have been accomplished. The obtained results confirmed that the application of the EHD technique for the investigated tube and electrode arrangement caused significant increase in heat transfer coefficient. The condensation enhancement depends both on the geometry of the electrode system and on the applied voltage.

Keywords: Condensation; Electrohydrodynamic technique; Heat transfer enhancement; Enhanced tubes

*Corresponding Author. E-mail: d.butrymowicz@pb.edu.pl

Nomenclature

c_p	–	condensate specific heat
D_o	–	outside tube diameter
f_e	–	electrohydrodynamic force
f_1	–	electrophoretic force
f_2	–	electrostriction force
f_3	–	dielectrophoretic force
f_4	–	electrostriction force
g	–	gravitational acceleration
h_{fg}	–	specific enthalpy of vaporisation
s	–	distance between tube and electrode
T_s	–	saturation temperature
T_w	–	wall mean temperature
v	—	voltage

Greek symbols

α	–	heat transfer coefficient
Γ	–	condensate mass flow rate per unit length
ε_r	–	relative electric permittivity
ε	–	electric permittivity
Φ	–	flooding angle
λ	–	condensate thermal conductivity
ρ	–	condensate density
ν	–	condensate kinematic viscosity
ω	–	angle of position of the electrode

1 Introduction

Common thermohydraulic goals in thermal engineering are to reduce the size of a heat exchanger required for a specified heat duty, to upgrade the capacity of an existing heat exchanger, or to reduce the approach temperature difference for the process streams [1]. Heat transfer enhancement may be thought as a rational and effective approach to achieve these goals.

Generally one can consider two different enhancement techniques: passive and active ones. The passive techniques do not require the application of the external power, whereas the active techniques require activator or power supply to bring about the enhancement. Many passive and active augmentation techniques have been applied for vapor space condensation. In many cases, horizontal and vertical condensers found in power stations, refrigeration, organic Rankine cycles (ORC) and heat pumps devices as well as process industries involve condensation on the outside of tubes [3,4].

Surface extensions are widely employed for augmentation of condensa-

tion heat transfer. Horizontal integral-fin tubes of a high fin density are most commonly applied, especially for condensation of vapor other than steam, e.g., refrigerants. With proper geometry of the fins, the average film heat transfer coefficient can be several times that of a bare tube with the same base diameter. However, there is strong limitation of condensation heat transfer improvement due to capillary effects which play the principal role on condensate drainage from these tubes. Recent interest has been focused on the additional improvement of condensation heat transfer by means of application of three dimensional fins and/or using the effective methods of condensate drainage.

The paper concentrates on condensation heat transfer augmentation with use of active condensate drainage by means of strong electric field, but the based information concerning the condensation on horizontal finned tubes was also discussed.

2 Condensation on horizontal finned tubes

The most important phenomenon during condensation on low profile horizontal integral-fin tube is the so-called Gregorig effect which is caused by the surface tension forces [4,5]. The liquid film at the top of the fin is convex whereas at its base is concave. Therefore the pressure within the liquid phase is greater at the fin top and lower at the fin base in comparison with the pressure of the vapor. This leads to the pressure gradient along the fin flank which reduces the liquid film thickness. This phenomenon is called as the Gregorig effect. Due to this effect very high heat transfer coefficient for horizontal integral-fin tubes can be achieved.

It is well known that when a highly wetting liquid comes in contact with a horizontal finned tube, surface tension force will cause the liquid to be retained between the fins at the bottom of the tube. This is the unfavourable effect caused by capillary forces. Condensate retention between the fins have been studied by many investigators, e.g., Honda *et al.* [6], Rudy and Webb [7]. The flooding may be characterized by the so-called flooding angle, Φ, which is measured from the top of the tube to a position where the inter-fin spaces are just completely filled with the condensate. The flooding angle depends mainly on the tube geometry and the capillary constant. Based on their own results, Webb *et al.* [8] found out that the heat transfer rate across the zone of retained condensate was negligible for most practical cases. Thus, reducing of the condensate retention can be

thought as the very effective method of condensation heat transfer augmentation [9].

Condensation process usually occurs in bundles of horizontal tubes. In these cases there is the additional complication since condensate flows from higher or upstream tubes falling on lower or downstream tubes. The condensate inundation leads to thicker condensate films on the inundate tubes. Due to this effect the average film heat transfer coefficient for the tube bundle is significantly lower in comparison with condensation on single horizontal finned tube.

Works have been done to define the flow patterns that exist on a bank of integral-fin tubes. Honda *et. al* [10] were able to predict the condensation coefficient on a bank of integral-fin tubes. According to Honda *et al.* [10] the condensate leaves the tube bottom as a liquid jet (Fig. 1). Next, the condensate spreads axially over a few interfin channels only, creating a condensate affected region (B). Between two affected regions it may be assumed that the condensation process is not affected by the condensate inundation. Experimental investigations showed also that for the bundles consisting of the integral-fin tubes the inundation causes lower heat transfer deterioration in comparison with the case of the bundle of bare tubes [3].

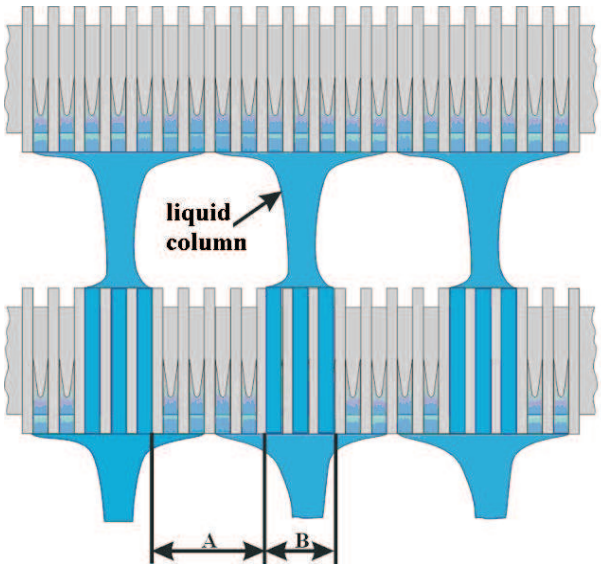

Figure 1: The condensate flow pattern according to Honda *et al.* [10]: A – unaffected region of vapor condensation, B – affected region by condensate inundation.

3 Electrohydrodynamic condensate drainage

The physical basis of enhanced condensation due to the electrohydrodynamic (EHD) force generated by an electric field is given by equation [11]

$$f_e = qE - \frac{1}{2}E^2\nabla\varepsilon + \frac{1}{2}\nabla\left[E^2\left(\frac{\partial\varepsilon}{\partial\rho}\right)_T\rho\right] , \tag{1}$$

where q is the electric charge density, E is the electric field strength, ε is the electric permittivity, ρ is the condensate density and subscript T denotes temperature.
It may be further written in a more detail at form for non-polar fluids [11] as:

$$\begin{aligned} f_e = f_1 + f_2 + f_3 + f_4 = qE - \frac{1}{2}E^2\nabla\varepsilon + \\ + \frac{1}{6}\varepsilon_o\left(\varepsilon_r - 1\right)\left(\varepsilon_r + 2\right)\nabla E^2 + \frac{1}{6}\varepsilon_o E^2\nabla\left[\left(\varepsilon_r - 1\right)\left(\varepsilon_r + 2\right)\right] , \end{aligned} \tag{2}$$

where ε_o and ε_r denote electric permittivity of free space, and relative permittivity, respectively. The first component represents the electrophoretic force, f_1, exerted by an electric field upon electric charges in the fluid. The second component, f_2, comes from the spatial distribution of electric permittivity ε which is not caused by electrostriction. This component acts perpendicularly to the inter-phase surface from the material of higher permittivity (liquid) to the material of lower permittivity (vapor). This component acts to disturb the condensate film. The third component, f_3, is dielectrophoretic force which is due to the nonuniformity of the electric field. This force pushes condensate towards higher electric field strength. The last component, f_4, is the electrostriction force, which occurs whether or not an applied field is uniform. This force depends on nonuniformity of electrical permittivity. In the case of film condensation this component is significant at the interphase surface only when abrupt change of ε_r occurs. The direction of this force is the same as direction of increasing permittivity (from vapor to liquid) and perpendicular to the interphase surface. It may be suggested that in most cases the spatial distribution of the electric permittivity, ε, plays the dominant role for dielectric fluids.

Velkoff and Miller [14] first reported the effect of electric field on condensation heat transfer in 1965. They quoted the increase of the mean heat transfer coefficient by about 200% during condensation of refrigerant R-113 on a flat, vertical plate upon the application of an intense electric field

perpendicular to the plate. Experimental investigations of electrohydrodynamic (EHD) enhanced condensation heat transfer have been carried out by many other researches, for example: Choi [15], Holmes and Chapman [16], Seth and Lee [17]. In all these cases, the condensation enhancement was found to be caused by an electrically induced destabilisation of the condensate film. Very interesting investigation has been done by Didkovsky and Bologa [18,19]. They obtained EHD enhancement as much as 20 times during condensation on the smooth vertical tube. It should be mentioned that most investigations deal with the condensation augmentation by application of the electric field to vertical plates or vertical tubes [13]. The electric field is usually generated by means of coaxial rod and mesh electrodes. The condensate is drained just from the heat transfer area as it is shown in Fig. 2.

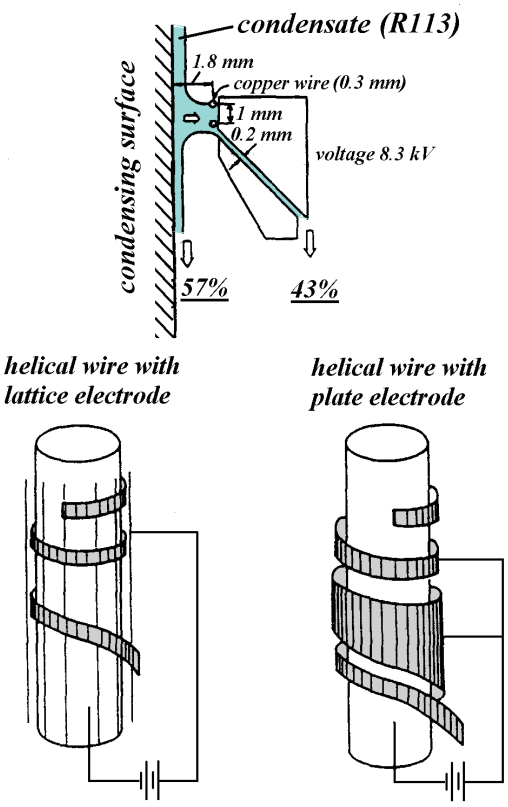

Figure 2: Condensation heat transfer enhancement on vertical tubes [12].

It is worth to note that the very limited data on EHD condensation enhancement exist for horizontal tubes, especially for the finned ones. Allen and Karayiannis concluded [13], basing on their own experimental investigation, that in the case of horizontal smooth tube (Fig. 3) even the best EHD-assisted performance falls short of that given by using a single integral-fin tube without any active heat transfer augmentation. Thus the idea of using strong electric field to enhance heat transfer in the case of smooth horizontal tube seemed to be a questionable problem. Allen and Karayiannis also claimed [13] that for the horizontal integral-fin tube with the coaxial electrode the EHD enhancement is negligibly small. They suggested that the phenomena caused by the surface-tension forces play the dominant role also in this case.

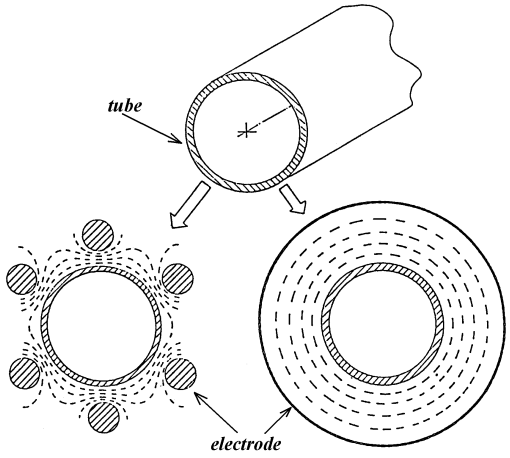

Figure 3: Distributions of equipotential lines for horizontal smooth tube fitted with system of rod electrodes and fitted with mesh concentric electrode, [13].

It is quite obvious that when the strong coaxial electric field is applied to the integral-fin tube the EHD forces act against the surface tension forces, i.e., pulling out the condensate thus reducing the positive Gregorig effect. Therefore it is not now surprising, as claimed by Cooper [20], that the EHD assisted condensation enhancement applied to the horizontal integral-fin tube is negligible. It should be stressed that this conclusion is valid only for the case when the coaxial electric field caused by the use of coaxial wires or coaxial mesh electrode system is used (Fig. 3). The above conclusions shed more light on the EHD condensation mechanism and are very helpful in

formulation of a new active method for EHD enhancement of condensation on the horizontal integral-fin tube [24]. This method is presented in a very short manner below.

Due to the condensate flow induced by the EHD forces, a significant area of the tube surface remains unflooded, thus making favourable conditions for condensate heat transfer. In other words the proper application of the EHD condensate drainage shell lead to an increase of the so-called flooding angle, Φ – a parameter which clearly defines the area of the finned tube free from the retained condensate.

The idea of the EHD condensate drainage enhancement [21] technique is illustrated in Fig. 4. The main feature of it is represented by the ar-

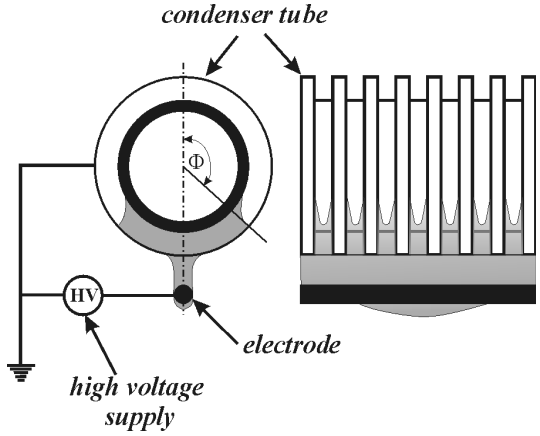

Figure 4: The idea of the condensation enhancement by EHD condensate drainage.

rangement of the tube – electrode system. In this case the electric field is generated between the rod-type electrode and the lower part of the finned tube. Therefore, taking into account the EHD mechanism one may expect that the majority of the tube surface is not affected by the electric field with the exception of the small part of it at the tube bottom. As it is depicted above, this part usually plays a minor role in heat transfer also without the electric field since the interfin spaces are usually flooded totally by the condensate. Thus there are two positive phenomena with respect to heat transfer augmentation in the considered case. The first one follows from the Gregorig effect which takes place in the upper part of the tube (not disturbed by the EHD forces) and second one is due to the EHD forces pulling down the condensate from the bottom of the tube. It is seen that

in this method the EHD forces act only on the condensate drainage process and not on the condensation phenomenon itself.

4 Experimental apparatus and procedure

The main goal of the experimental investigations was to provide the data to confirm the theoretical expectations of EHD condensation enhancement according to the idea shown in Fig. 4. The experimental investigations reported below covered measurements of the heat transfer coefficient during condensation of refrigerant R-123 at the average saturation temperature 313.15 K; for various configurations and the geometries of the drainage electrodes with single tube. The modified Wilson plot technique was used in these experiments in the form similar to that of Briggs and Young [22]. The detailed description of the experimental rig, the measurement procedure and data reduction one can find in [21]. The dimensions of the investigated tubes are given in Tab. 1. The rod-type electrodes were made of brass. For a reference purpose the heat transfer measurements were done for smooth tubes of the same outer diameter.

Table 1: Geometry of the investigated finned tubes.

Tube	Unit	1	2	3	4	5	6
fin density	fin/m	–	1030.9	–	757.6	–	1851.7
inner diameter	mm	13.0	11.02	15.60	13.8	13.0	13.0
fin root diameter	mm	–	13.41	–	16.16	–	15.2
outer diameter	mm	16.0	16.17	18.76	18.76	16.0	16.0
fin pitch	mm	–	0.97	–	1.32	–	0.54
fin height	mm	–	1.38	–	1.30	–	0.40
fin thickness at fin root	mm	–	0.40	–	0.46	–	0.27
fin thickness at fin top	mm	–	0.21	–	0.29	–	0.27
material	–	copper	copper	nickeline	nickeline	brass	brass

An experimental investigation was conducted on the test rig depicted in Fig. 5. Experiments covered determination of the heat transfer coefficient during condensation of refrigerant R-123 at the average saturation temperature 313.15 K.

The test apparatus consists of two main elements: condenser 1 with a tested tube 2 mounted inside it and a vapor generator 14. The length of the test section is 1.0 m. The condenser is equipped with six glass windows.

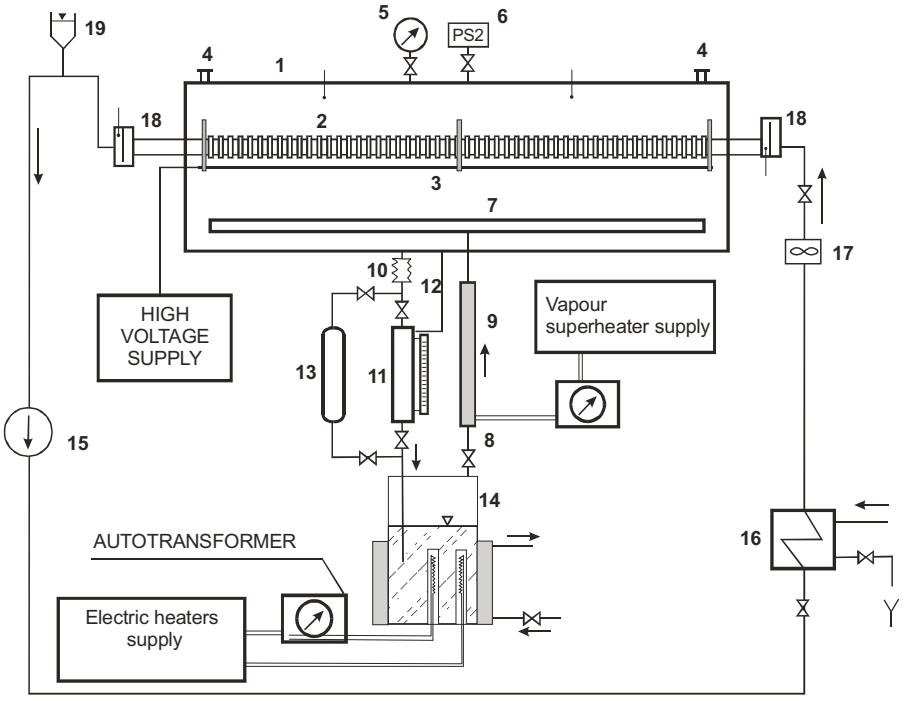

Figure 5: Schematic diagram of the test apparatus: 1 – condenser, 2 – tested tube, 3 – electrode along with insulation grips, 4 – air purging valve, 5 – mano-vacuum meter, 6 – pressure transducer, 7 – vapor supply pipe (inside condenser), 8 – vapor supply line, 9 – vapor superheater, 10 – condensate outflow tube, 11 – condensate calibrating tank, 12 – levelling line, 13 – dehydrator, 14 – vapor generator with cooling jacket, 15 – cooling water pump, 16 – heat exchanger, 17 – turbine water flow rate meter, 18 – water temperature measurement tank, 19 – air purging valve of cooling water system.

The test apparatus contains a calibrating tank 11 to measure the condensate flow rate and dehydrator 13 filled with molecular sieves of the type 4A. The condensate flows down from the tested tube to the tank 11 and then to the vapor generator 14 equipped with electric heaters. The high voltage was delivered to the electrode by sparking plug mounted at the backside of the condenser. The following quantities were measured in the course of the investigations:

- inlet water temperature – in tank 18 and at the inlet of the test section;
- outlet water temperature – in tank 18 and at the exit of the test section;

- vapor temperature – at two points inside condenser;
- vapor pressure – by the use of pressure transducer of accuracy class 0.1;
- water flow rate by the use of turbine flow meter of accuracy class 1.0;
- volume of condensate – in the calibrating tank 11;
- time of fill up of the tank 11.

All temperatures were measured by means of the thermocouples of the type K using the electronic measurement system. The measuring error was estimated as ±0.15 K. The data were recorded once the steady state was achieved. Basically from all data points the only ones were taken into account when the difference of the heat fluxes calculated from the heat balances on water and on the vapor sides did not exceed 15%. For most data points this difference was below 5% owing to the careful measurement and appropriate scaling of the whole test rig. The condensation heat transfer coefficient was determined by means of the Wilson plot technique [21].

5 Results for single electrode drainage

Film heat transfer coefficient, α, is based on the surface area of the smooth tube of the diameter of the fin tips. The measured condensation heat transfer coefficients are compared in Tab. 2 against the values of the heat transfer coefficient, α_{Nu}, for the smooth tube of the same outer diameter calculated from the well known analytic Nusselt formula [23],

$$\alpha_{Nu} = 0.728 \left[\frac{\lambda^3 \rho g h_{fg}}{\nu \left(T_s - T_w\right) D_o} \left(1 + \frac{3}{8} \frac{c_p \left(T_s - T_w\right)}{h_{fg}} \right) \right]^{\frac{1}{4}} , \qquad (3)$$

and the measured heat transfer coefficient, α_o, for the finned tube without the EHD condensate drainage enhancement.

The experimental results for tubes Nos. 1 and No. 2 are presented in Fig. 6. The application of the voltage of 25.0 kV caused the increase of the condensation heat transfer coefficient by 27%. The total increase of the heat transfer coefficient due to both surface area and EHD enhancement in comparison with the bare tube was found to be 4.7 times.

The observation of the condensation phenomenon proved that the amount of the retained condensate between the fins was reduced by the EHD effect almost completely. In this case the value of the flooding angle is $\Phi_e/\pi \approx 1.0$.

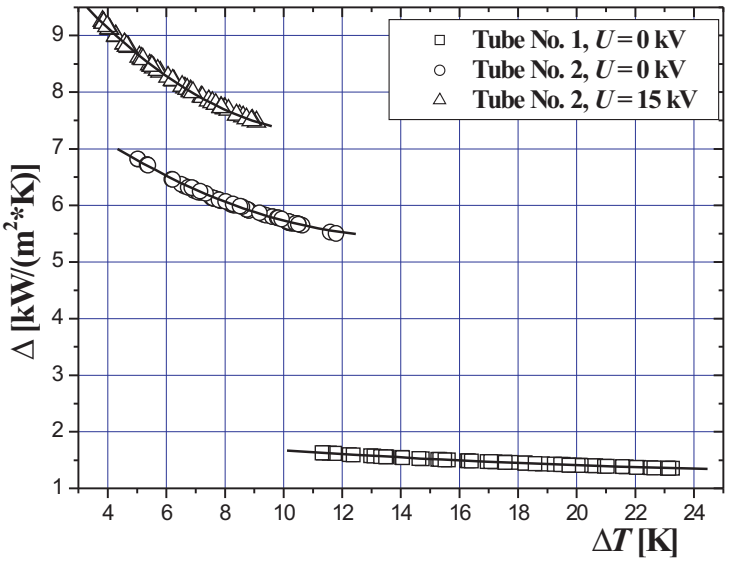

Figure 6: Results of the experimental investigations of tube Nos. 1 and 2, $U = 15$ kV.

The theoretical value of the flooding angle calculated with the drainage parameter $\chi_d = 0$ gives $\Phi/\pi = 0.74$ and estimated value from the photograph is equal to $\Phi/\pi = 0.78$. Basing on these results one can estimate theoretical increase of the condensation heat transfer coefficient due to elimination of the condensate retention as $\alpha_e/\alpha = \Phi_e/\Phi = 1.00/0.78 = 1.28$ which agrees very well with the experimental results (the subscript e denotes here the EHD drainage).

The experimental results obtained for tube Nos. 4 and 6 are presented in Figs. 7 and 8, respectively. It is evident that the condensation enhancement can significantly reduce mean temperature difference, ΔT, between saturated condensing vapor and the outer surface of the tube. For example, this temperature difference may be reduced as much as three times for the EHD condensation enhancement for tube No. 2 and almost six times for Tube No. 4 in comparison with the smooth tubes of the same diameter. Since for the refrigeration or heat pump cycles the temperature difference ΔT in the condenser may be considered as a part of the total temperature difference between the heat source and the heat sink then the significant decrease of ΔT due to the heat transfer enhancement by the EHD method leads to the strong increase of the cycle efficiency.

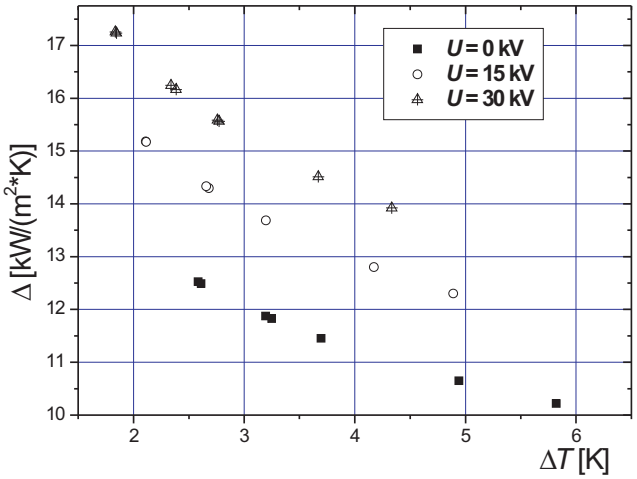

Figure 7: Results of experimental investigations of tube No. 4 for various voltages applied.

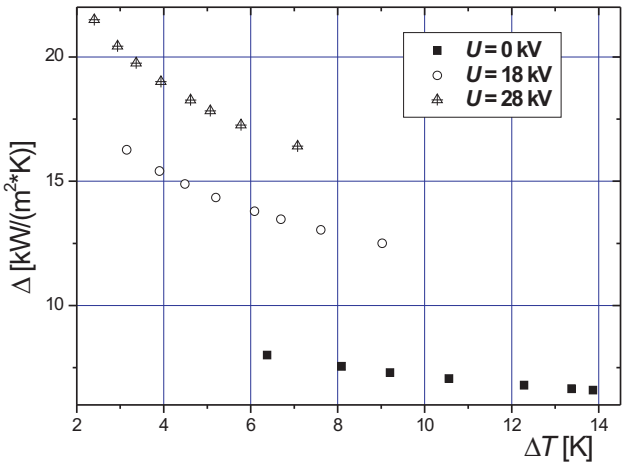

Figure 8: Results of experimental investigations of tube No. 6 for various voltages applied, electrode of the diameter 5.0 mm.

The very important role in the investigated phenomenon plays the flow pattern of the condensate leaving the tube [24]. The condensate flow patterns for tube Nos. 2 and 4 are shown in Figs. 9 and 10, respectively. They

are the same for the given range of the condensate mass flow rate, Γ, and the applied voltage, V.

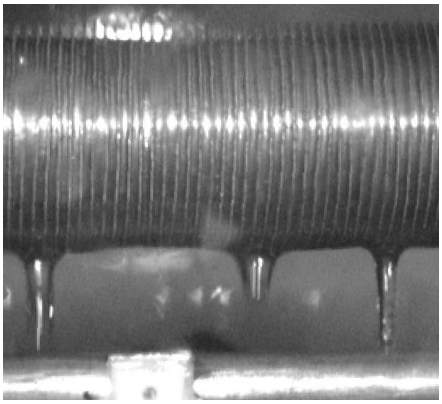

a) $U = 0$ kV, droplet mode

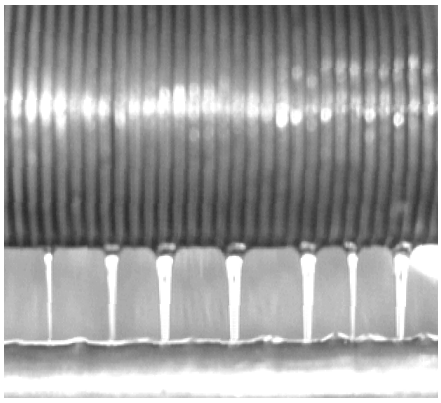

b) $U = 10$ kV, jet mode

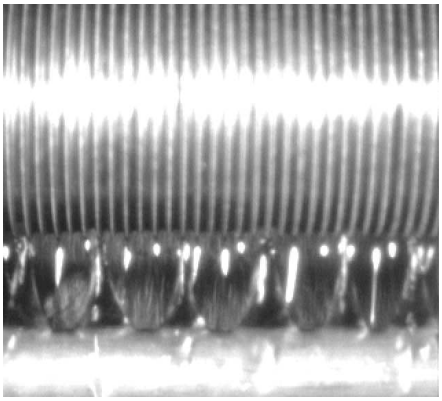

c) $U = 15$ kV, jet-cone mode

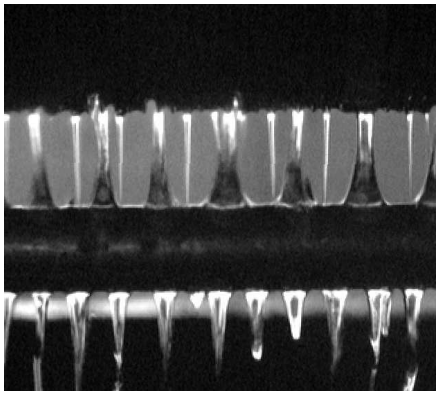

d) $U = 15$ kV, jet-cone mode silhouette

Figure 9: The condensate flow pattern for tube No. 2: a) $U = 0$, $\Gamma = 9.5$–19.3×10^{-3} kg/(m s); b) $U = 10$ kV, $\Gamma = 11.4$–22.7×10^{-3} kg/(m s); c) $U = 15$ kV, $\Gamma = 11.6$–22.2×10^{-3} kg/(m s).

It is very important to note, that the condensate flow patterns observed for tube No. 2 (Fig. 9d) were slightly different in comparison with tube No. 4 (Fig. 10d). In the latter case the condensate jet was formed from each fin tip. Therefore the jet spacing was the same as the fin pitch. In the case of Tube No. 2 the jet spacing was sufficiently larger than the fin pitch. This may be attributed as the main reason for such significant improvement of condensation heat transfer measured for tube No. 4.

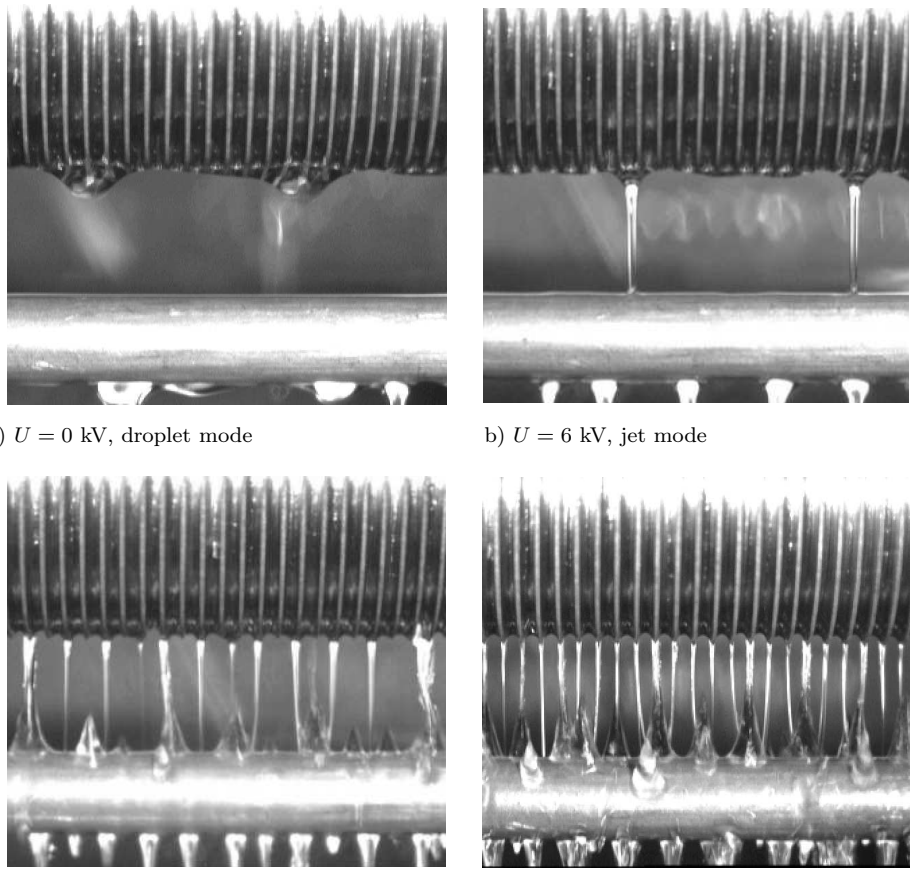

a) $U = 0$ kV, droplet mode

b) $U = 6$ kV, jet mode

c) $U = 16$ kV, jet-cone mode

d) $U = 22$ kV, jet-cone mode

Figure 10: The condensate flow pattern for tube No. 4: a) $U = 0$, $\Gamma = 7$–14.6×10^{-3} kg/(m s); d) $U = 22$ kV, $\Gamma = 7.5$–18.3×10^{-3} kg/(m s).

The schematic diagram of the observed flow patterns of the condensate leaving the tube is presented in Fig. 11. Four distinguished modes were observed: drop, jet, cone and a curtain mode. The drop mode occurred in the absence of the electric field. For medium voltage the jet mode was formed. Next the cone mode appeared. As the voltage further increased, the cones became bigger – see Fig. 11c and Fig. 11d. For the highest electrode potential the curtain mode may develop.

Approximately 60% increase of condensation heat transfer coefficient is possible by means of the application of a sharp-edge electrode – Fig. 13.

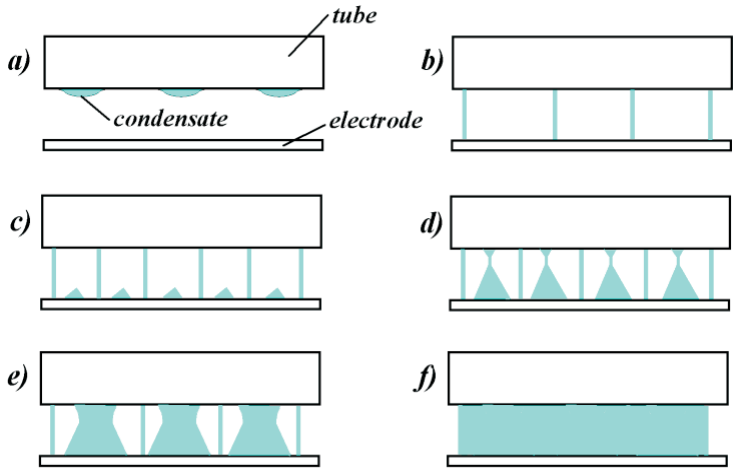

Figure 11: Schematic diagram of flow patterns for condensate leaving the tube – the effect of increase of the electrode potential for the rod-type electrode: a) drop mode, b) jet mode, c), d), e) jet-cone mode, f) curtain mode.

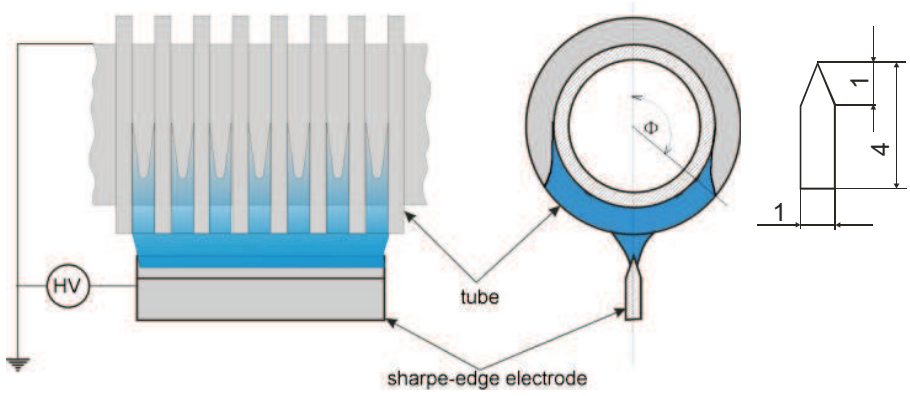

Figure 12: Electrohydrodynamic condensate drainage by means of a sharp-edge electrode: a) physical situation, b) geometry of the electrode given in mm.

The distance between the electrode and tested tube was $s = 6.6$ mm in the presented case. The condensate flow patterns in this case are presented in Fig. 14. As the voltage applied increased, the flow patterns changed from droplet mode, through jet to curtain mode.

The investigations covered also measurements of the effect of axisymmetric electric field on condensation process on horizontal finned tube [21].

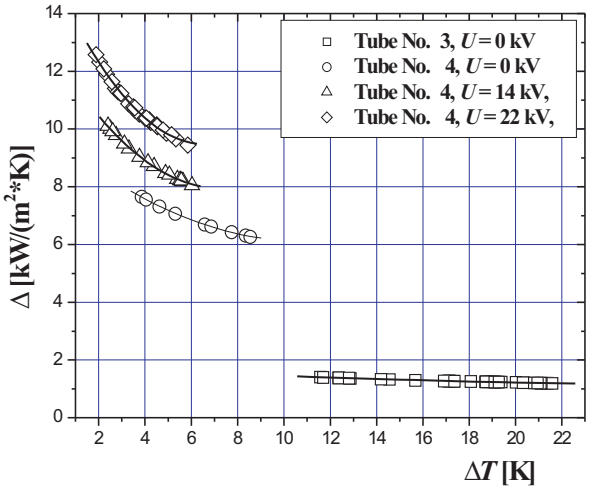

Figure 13: Results of the experimental investigations of tube Nos. 3 and 4 fitted with the sharp-edge electrode [21].

The electric field was generated in this case by a special concentric electrode (Fig. 15).
For the case of finned tube No. 2 application of the concentric electrode caused decrease of heat transfer coefficient by as much as 14% (Fig. 16). The observation of the condensate flow patterns (Fig. 17) proved that the certain amount of the condensate was removed from the space between fins at the upper part of the tube as an effect of the EHD forces. The action of the EHD forces disturbed then the Gregorig effect which resulted in decrease of the heat transfer coefficient.

6 Electrohydrodynamic condensate drainage double electrode system

In many cases under high electric voltage the condensate jet pitch is equal to fin pitch which can be thought as unfavourable case bearing in mind the condensate inundation phenomenon. Thus, the EHD condensate drainage may change the condensate inundation in the tube bundle. This is the reason why the additional studies should be carried on in order to find out the effective techniques of EHD condensate drainage organisation. The idea of electrode geometry presented before was based to our modification which is presented in Fig. 18. Two electrodes connected in parallel form a double

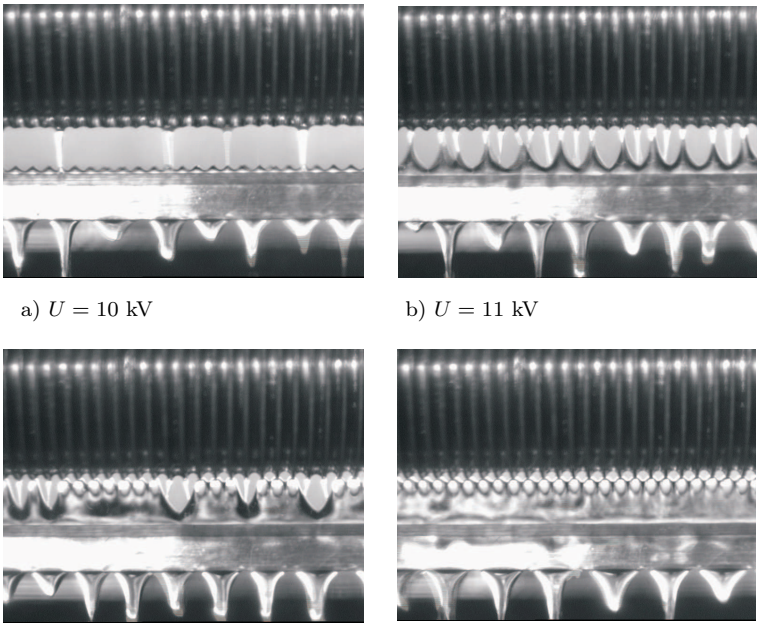

a) $U = 10$ kV b) $U = 11$ kV

c) $U = 12$ kV d) $U = 14$ kV

Figure 14: Condensate flow patterns from tube No. 4 equipped with the sharp-edge electrode.

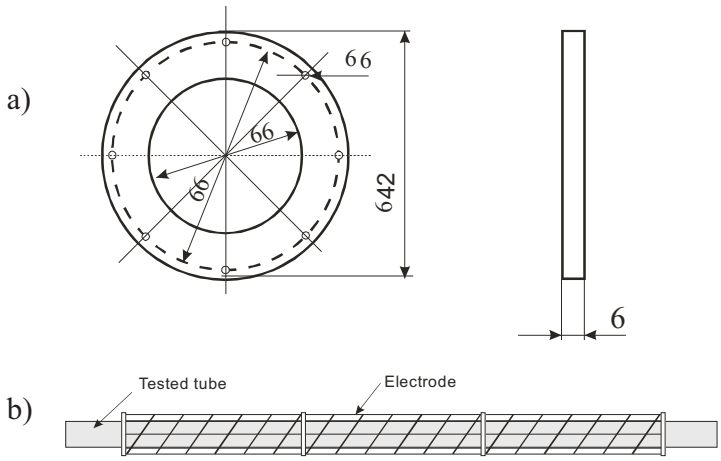

Figure 15: Geometry of a concentric electrode: a) polytetrafluorethylene (PTFE) distance rings; b) tube fitted with the electrode.

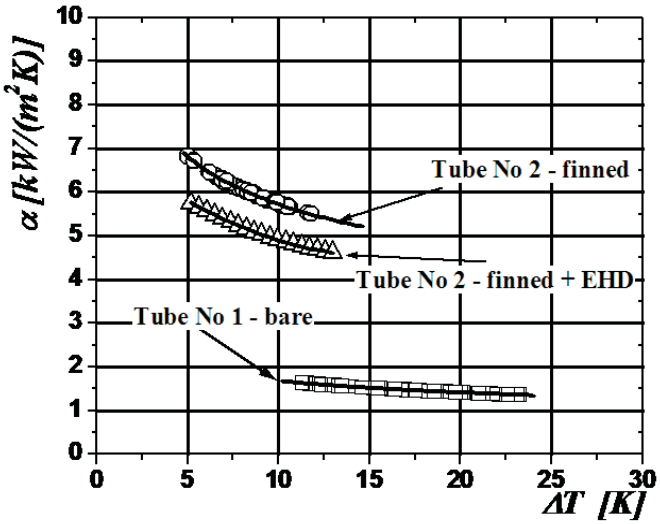

Figure 16: Results of investigations of finned tube No. 2, $U = 25$ kV, the concentric electrode.

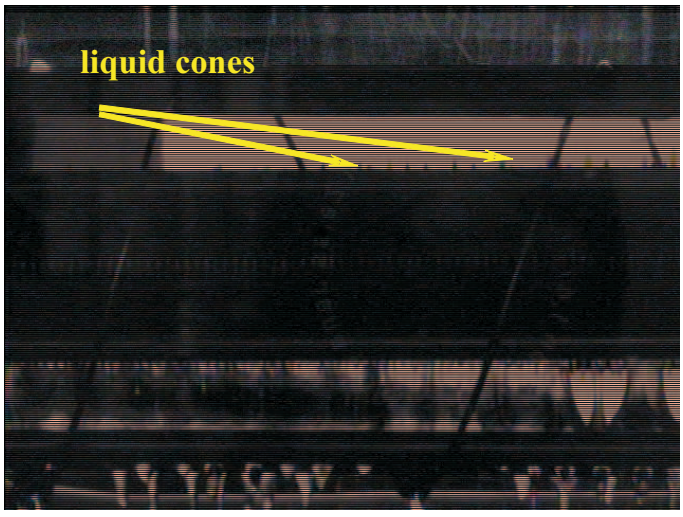

Figure 17: Silhouette of the condensate flow pattern on tube No. 2 equipped with the concentric electrode.

electrode. Due to the electric field the condensate is pulled towards the electrodes. The electrodes are interspaced between the tube bottoms in the tube bundle as it is depicted schematically in Fig. 19.

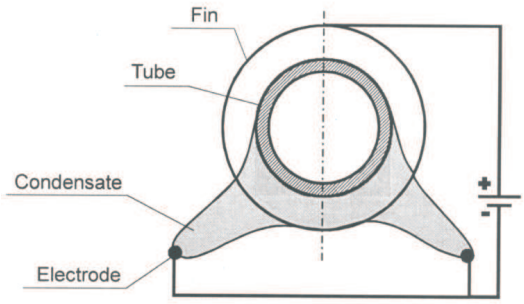

Figure 18: The idea of the EHD condensate drainage by means of the double electrode system.

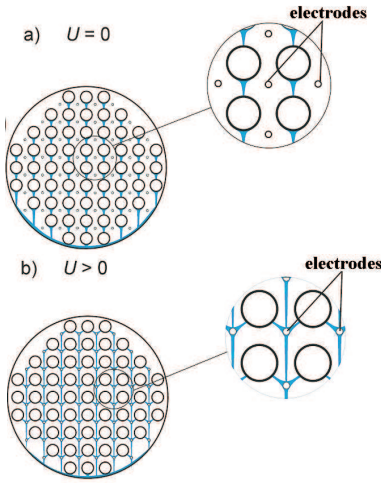

Figure 19: Schematic diagram of condensate flow pattern in bundle of horizontal tubes: a) without EHD drainage ($U = 0$ kV), b) with EHD drainage ($U > 0$ kV).

The experimental investigations covered the determination of condensation heat transfer coefficient for two finned tubes under conditions of the EHD condensate drainage as well without it. For a reference purpose the heat transfer measurement was done for bare tubes of the same outer diameter. The dimensions of the investigated tubes are given in Tab. 2. The electrodes were made of brass rods of the diameter 3.0 mm.

Three various geometries of the electrode systems were investigated for tube No. 6. The geometry of the tube-electrode system is shown in Fig. 20. Results of the heat transfer coefficient investigations are given in Tab. 3.

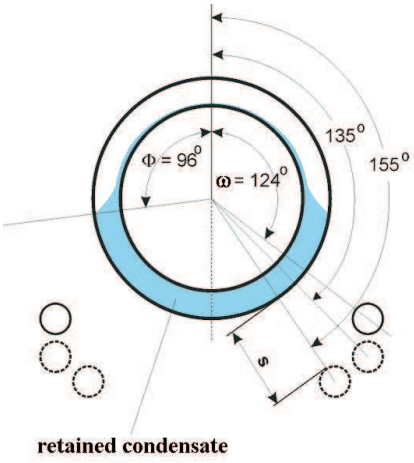

Figure 20: Geometry of the tube-double electrode systems. The angle Φ denotes the flooding angle (corresponding to the tube circumference free of the retained condensate) for tube No. 6.

Table 2: Results of heat transfer investigations with rod-type electrodes.

Tube	U [kV]	s [mm]	d_e [mm]	α/α_{Nu}	α/α_o	measurement error [%]
No. 1	0	–	–	0.98	–	7.5
No. 2	0	9.5	5.0	3.71	1.00	11.0
	25			4.71	1.27	10.0
No. 3	0	–	–	1.10	–	9.5
No. 4	0	9.0	3.0	6.04	1.00	15.7
	15			6.96	1.15	22.0
	30			7.64	1.27	18.0
No. 5	0	–	–	1.10	–	6.5
No. 6	0	5.0	5.0	4.63	1.00	6.5
	18			7.88	1.70	8.8
	28			9.73	2.10	8.7
	0	5.0	3.0	4.65	1.00	
	15			6.46	1.39	

On the basis of these results it is possible to conclude that heat transfer augmentation due to the condensate drainage strongly depends on both the electrodes distance, s, from the tube as well as the angle, ω, at which the electrodes are placed.

Table 3: Results of heat transfer investigations for the double electrode system.

Tube	U [kV]	s [mm]	ω [deg]	α/α_{Nu}	α/α_o	measurement error [%]
No. 6	0	4.9	124	5.61	1.00	3.3
	14			6.32	1.13	4.9
	0	7.5	135	5.39	1.00	5.3
	25			8.71	1.62	5.3

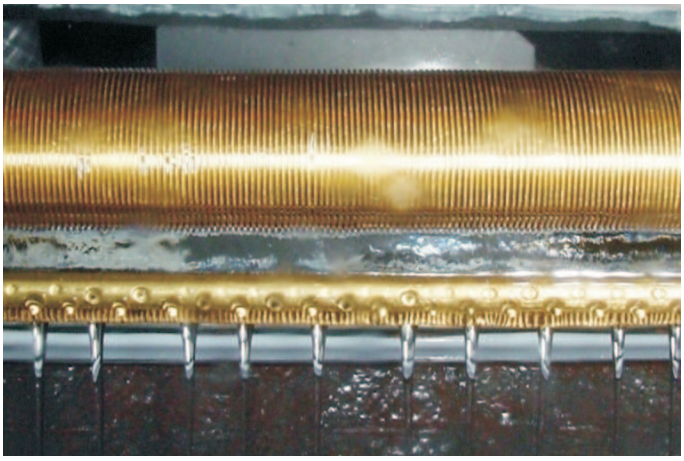

Figure 21: The condensate flow pattern between the tube and the electrode, tube No. 6, $\omega = 135^{\circ}$.

The heat transfer augmentation for tube No. 6 strongly depends on the angle ω. In the case of $\omega = 124^{\circ}$ the electrodes were placed close to the border between the retention zone (Fig. 20). In order to achieve the high heat transfer augmentation the distance s between the electrodes and the tube was adjusted to the smallest one. Because of the small distance between the electrodes and the tube, there was not possible to apply voltage greater than 14.0 kV. The best heat transfer augmentation was achieved for $\omega = 135^{\circ}$. The condensate flow patterns were observed during heat transfer investigations. In the case of the angle $\omega = 135^{\circ}$ (Fig. 21) the condensate flow pattern was still unchanged and liquid curtain was formed between the electrode and tube.

7 Conclusions

This paper has given a short overview of enhanced condensation technology by applying both passive and active techniques. The active technique of condensation enhancement may be achieved by applying the electrohydrodynamic condensate drainage augmentation. The performed experimental investigations proved the usefulness of the new idea of condensation heat transfer enhancement by EHD condensate drainage. The effectiveness of this method depends on the geometry of the tube as well as on the applied electrode potential. The enhancement of heat transfer coefficient ranges from 27% up to 110%. The average temperature difference between condensing vapor and outside tube wall for finned tube applied with the EHD condensate drainage was reduced as much as three or six times in comparison with the bare tube without the EHD effect.

Application of axisymmetric electric field generated by special concentric electrode caused decrease of heat transfer coefficient for finned tube as a result of disturbing the Gregorig effect. The effective condensation heat transfer augmentation by means of EHD condensate drainage requires careful analysis of the optimum geometry of the tube-electrodes system. The new arrangement of the tube-double electrode system was proposed in the paper which may be thought as the most suitable for the case of the bundle of horizontal tubes.

The heat transfer augmentation depends on both the angle ω at which the electrodes are placed, the voltage and the distance between the electrodes and the tube. On the basis of the experiments of condensation heat transfer it may be concluded that the optimum angle ω exists in respect to the heat transfer augmentation. It occurs that if the angle ω is lower than the flooding angle Φ then the heat transfer augmentation is smaller. However, if the angle ω is too large, then the unfavourable influence between the two electrodes occurs what diminishes the condensate drainage effect. The experimentally obtained heat transfer augmentation due to EHD condensate drainage by means of the double electrode system in the case of the investigated tube for the optimum angle $\omega = 135^{\circ}$ was found to be 62% in comparison with the same tube without EHD condensate drainage.

One may expect that the proposed tube-electrode arrangement should be very effective under conditions of condensation in the horizontal tubes bundle. However, this requires additional experimental verification.

Received 28 May 2012 and in revised form 30 October 2014

References

[1] Hewitt G.F. (Ed.): *Handbook of Heat Exchanger Design*, Begell House, New York 1992.

[2] Bergles A.E.: *Heat transfer enhancement – the encouragement and accommodation of high heat fluxes*. T. ASME, J. Heat Trans. **119**(1997), 8–19.

[3] Webb R.L.: *Principles of Enhanced Heat Transfer*, John Wiley and Sons, New York 1994.

[4] Marto P.J.: *An evaluation of film condensation on horizontal integral-fin tubes*. T. ASME J. Heat Trans. **110**(1988), 1287–1305.

[5] Gregorig R.: *Hautkondensation an feingewellten Oberflächen bei Berücksichtigung der Oberflächenspannungen*. Z. Angew. Math. Phys. **5**(1954), 36–49.

[6] Honda H., Nozu S., Mitsumori K.: *Augumentation of condensation on horizontal finned tubes by attaching a porous drainage strip*. In: Proc. ASME-JSME Thermal Eng. Joint Conf. (Y. Mori and W.-J. Yang, Eds.) **3**(1983), 289–296..

[7] Rudy T.M., Webb R.L.: *An analitycal model to predict condensate retention on horizontal integral-fin tubes*. T. ASME J. Heat Trans. **107**(1985), 361–368.

[8] Webb R.L., Rudy T.M., Kedzierski M.A.: *Prediction of the condensation coefficient on horizontal integral-fin tubes*. ASME J. Heat Transfer,**107**(1985), 369–376.

[9] Butrymowicz D., Trela M., Karwacki J.: *Enhancement of condensation heat transfer by means of passive and active condensate drainage techniques*. Int. J. Refrig. **26**(2003), 473–484.

[10] Honda H., Nozu S., Takeda Y.: *A theoretical model of film condensation in a bundle of a horizontal lowfinned tubes*. T. ASME, J. Heat Trans. **119**(1989), 2, 525–532.

[11] Yu Z., Al.-Dadah R.K., Winterton R.H.S.: *A theoretical investigation of electrohydrodynamically (EHD) enhanced condensation heat transfer*. In: Proc. Int. Con. Two-Phase Flow Modeling and Experimentation, Pisa 1999, **1**, 463–472.

[12] Tanasawa I.: *Recent advances in condensation heat transfer*. In: Proc. Int. Heat Transfer Conf., Brighton 1994, **1**, 297–312.

[13] Allen P.H.G., Karayiannis T.G.: *Electrohydrodynamic enhancement of heat transfer and fluid flow*. Heat Recov. Syst. CHP **15**(1995), 5, 389–423.

[14] Velkoff H.R., Miller J.H.: *Condensation of vapor on a vertical plate with a transverse electrostatic field*. T. ASME, J. Heat Trans. (1965), 197–201.

[15] Choi H.Y.: *Electrohydrodynamic condensation heat transfer*. T. ASME, J. Heat Transf. (1968), 98–102.

[16] Holmes R.E., Chapman A.J.: *Condensation of Freon-114 in the presence of a strong nonuniform alternating electric field*. T. ASME, J. Heat Trans. (1970), 616–620.

[17] Seth A.K., Lee L.: *The effect of an electric field in the presence of noncondensable gas on film condensation heat transfer*. T. ASME, J. Heat Trans. (1974), 257–258.

[18] Didkovsky A.B. Bologa, M.K.: *vapor film condensation heat transfer and hydrodynamics under the influence of an electric field*. Int. J. Heat Mass Trans. **24**(1981), 5, 811–819.

[19] Bologa M.K., Korovkin V.P., Savin I.K.: *Mechanism of condensation heat transfer enhancement in an electric field and the role of capillary processes*. Int. J. Heat Mass Trans. **38**(1995), 1, 175–182.

[20] Cooper P.: *Practical design aspects of EHD heat transfer enhancement in evaporators*. ASHRAE Trans. **98**(1992), 2, 445–454.

[21] Butrymowicz D., Karwacki J., Trela M.: *Investigation of condensation on horizontal tubes with electrohydrodynamic condensate drainage*. Rep. IFFM PAS 523/1482/2002, Gdańsk 2002 (in Polish).

[22] Briggs D.E., Young E.H.: *Modified Wilson plot techniques for obtaining heat transfer correlations for shell and tube heat exchangers*. Chem. Eng. Progres. Symp., Ser. 92, **65**(1969), 35–45.

[23] Madejski J.: *Theory of Heat Transfer*. Szczecin 1998 (in Polish).

[24] Butrymowicz D., Trela M., Karwacki J.: *Enhancement of condensation heat transfer by means of EHD condensate drainage*. Int. J. Therm. Sci. **41**(2002), 646–657.